ACS APPLIED MATERIALS & INTERFACES

Research Article

www.acsami.org

Thermally Induced Percolational Transition and Thermal Stability of Silver Nanowire Networks Studied by THz Spectroscopy

Jing-Zhi Chen, Hyeyoung Ahn,* Shin-Chun Yen, and Yao-Jiun Tsai

Department of Photonics, National Chiao-Tung University, Hsinchu 30010, Taiwan, Republic of China

Supporting Information

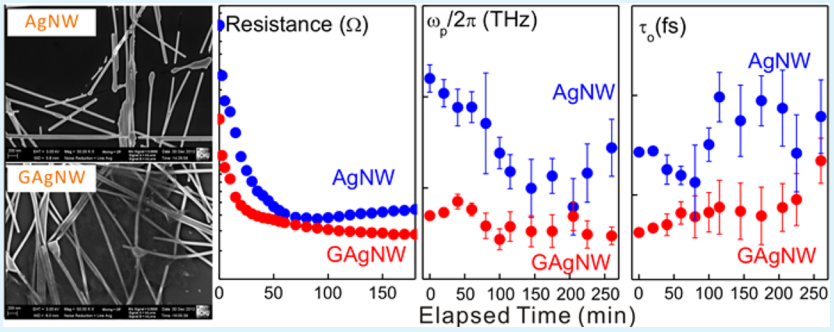

ABSTRACT: Great demand toward flexible optoelectronic devices finds metal nanowires (NWs) the most promising flexible transparent conducting material with superior mechanical properties. However, ultrathin metal nanowires suffer from relatively poor thermal stability and sheet conductance, attributed to the poor adhesivity of the ohmic contact between nanowires. Thermal heating and annealing at 200 °C increase the conductivity of the metal network, but prolonged annealing accelerates the breakage of NWs near the NW junction and the formation of Ag droplets. In this study, the thermal stability of silver NW (AgNW) films is investigated through the *in situ* measurements of sheet resistance and terahertz (THz) conductivity. With the improved ohmic contact at the NW junctions by heating, a characteristic transition from the subpercolative to percolative network is observed by *in situ* THz spectroscopy. It is found that stamp-transferred graphene incorporated with a near-percolative AgNW network can dramatically enhance the thermal stability of the graphene−AgNW (GAgNW) hybrid film. In both *in situ* measurements, little variation of physical parameters in GAgNW film is observed for up to 3 h of annealing. The presented results offer the potential of graphene-incorporated metal nanowire film as a highly conductive electrode that also has high thermal stability and excellent transparency for next-generation electronics and optoelectronics on flexible substrates.

KEYWORDS: *transparent electrode, silver nanowires, graphene, terahertz spectroscopy, thermal stability*

INTRODUCTION

Progress toward low-cost, flexible optoelectronic devices including flat panel or plasma displays and solar cells requires electrodes not only with high transparency and conductivity but also with mechanical and thermal stability. Due to their remarkable physical properties, metallic nanowires (NWs) emerge as the most promising alternatives to indium tin oxide (ITO). Percolatively connected Ag nanowire (AgNW) networks can be spin-coated or spray-casted over nearly any substrate at room temperature and show the potential for realization of cheap, flexible, and transparent electrodes.[1−7] Recently, a percolational transition from the insulating to conducting phase near the critical NW density (N_c) was observed for AgNW films.[8]

Due to the increase of electrical resistivity and the decrease of thermal conductivity related with the size effects on the nanoscale, external heating or self-heating (Joule heat) of AgNWs may cause melting of NWs at a much lower temperature than the melting temperature of bulk silver at $T \sim 960$ °C.[9,10] Moreover, in order to be integrated in solar cells and display devices, AgNW networks need to withstand a high fabrication temperature up to several hundred degrees Celsius. According to recent reports, the AgNW network can maintain its high electrical conductivity until it is heated up to ∼200 °C, and its conductivity can even be improved when local fusing of NW junctions is achieved by prolonged heating (annealing) of the metallic network at a submelting temperature for long periods of time.[11,12] Heating at $T > 200$ °C can cause the AgNW network to break at the nanowire junctions and subsequently form metal droplets.[13] The failure of electrical performance of AgNWs results in the performance degradation of metallic network-based devices. Therefore, the comprehensive understanding of long-term thermal stability of the AgNW network and the possible solutions to enhance the thermal stability are crucial issues for further development of AgNW-based devices.

Received: August 26, 2014
Accepted: November 17, 2014
Published: November 17, 2014

Graphene is known to have extremely high thermal conductivity (~3080−5150 W/m K) and high thermal stability.[13,14] These excellent thermal properties allow graphene to enhance the heat dissipating capability in various nanocomposites and hybrids.[15] Furthermore, the two-dimensional planar structure of graphene can help to achieve good adhesion on the AgNW network to prevent the penetration of gases or ambient humidity.[16,17] Pristine monolayer graphene has not only excellent electrical and thermal conductivity but also high optical transparency (~2.3% absorption per layer)[18] so that graphene itself can be one of the best alternative materials to ITO. In practice, however, those excellent characteristics of graphene have been achieved only for high quality graphene transferred by mechanical exfoliation, the process of which is expensive and unsuitable for large scale electronic devices. By integration with AgNWs, relatively poor quality graphene prepared by other transfer methods can dramatically improve the electrical and mechanical performance of graphene−AgNW (GAgNW) hybrid electrodes.[19,20] In the GAgNW hybrid films, the main conductive component can be either a graphene layer or metal network, depending on whether metal networks are subpercolative or percolatative.[17,21−24] Graphene multilayers or high density of AgNWs can be used to further enhance electrical conductivity, but in either case, the optical transparency can be significantly reduced. To overcome this problem, in this work, we fabricated GAgNW films by *stamp transferring* a monolayer graphene onto the precoated AgNW film with the NW density (N) very near to but slightly lower than the percolational threshold N_c. The evolution of electrical properties during the thermal heating and annealing processes are measured *in situ* by using THz time-domain spectroscopy (THz-TDS) and two-point probe techniques. THz spectroscopy has been proven to characterize the electrical conductivities of various materials. In particular, since it is an optical and noncontact method, THz-TDS can easily be integrated with various types of nanostructures to characterize their dielectric and transport properties. For thin conductive films, the frequency dependence of THz conductivity $\tilde{\sigma}(\omega)$ shows simple Drude behavior. For nanostructures, however, $\tilde{\sigma}(\omega)$ deviates from the Drude behavior, and this non-Drude THz conductivity has been successfully described by the Drude−Smith model, which includes the backscattering event due to the localization in nanostructures.[25] Our results show that despite poor coverage quality, stamp-transferred graphene can significantly improve both thermal stability and electrical conductivity of the graphene−(subpercolated)AgNW hybrid films, while keeping high optical transparency.

RESULTS AND DISCUSSION

AgNW films with subpercolation concentration (~0.06 wt %) were prepared by using a spin coating method on Si substrates, while GAgNW hybrid films were prepared by a dry process (stamp transfer) using a soft substrate, polyethylene terephthalate (PET), to transfer chemical vapor deposition (CVD)-grown pristine graphene to precoated AgNW films. The details of sample preparation procedures are shown in Figure S1. The separately measured N_c for AgNW films used in this work was ~0.075 ± 0.010 wt %.[26] Since some AgNWs can be lost during the transfer process, the actual NW density in the GAgNW film was slightly lower than 0.06 wt %. The optical transmittance spectra of AgNW and GAgNW hybrid samples are measured in the spectral range of 400−1500 nm and illustrated in Figure 1. The optical transmittance of GAgNW film decreases by 2−3% due to the single layer of graphene but is still higher than 95% in the whole visible and near-infrared region. The heat treatment process does not influence the optical transmittance of GAgNW films since it depends on the areal filling factor of NWs.[8]

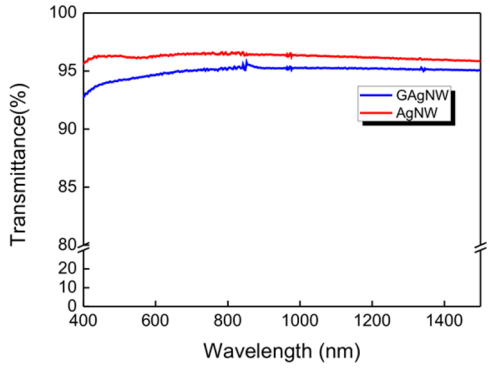

Figure 1. Optical transmittance spectra of AgNW and GAgNW films which are separately grown on glass substrates. The absorption due to the graphene layer is ≲2−3%, and in the spectral range of 500−1500 nm, the optical transmittance of GAgNW is higher than 95%.

The morphological evolution of the AgNW network during thermal treatment was investigated using a field emission scanning electron microscope (FE-SEM). The SEM images in Figure 2 show that AgNWs are randomly oriented without preferential direction and significant bundling of wires over the area of the substrate. As can be seen in Figure S2, stamp-transferred graphene does not fully cover the underlying AgNW film and may include the residual silicone gel, but its Raman spectrum clearly shows the characteristic peaks of single layer graphene at 1589 and 2687 cm^{-1}. In Figure 2d−f, the shaded areas in the images of GAgNW films correspond to the AgNWs covered by the graphene layer. The typical values of sheet resistance for AgNW (0.06 wt %) and GAgNW films before heating are measured to be 1500 ± 544 Ω/sq and 555 ± 309 Ω/sq, respectively. Figure 2a and d are SEM images of AgNW and GAgNW films after being heated from 25 to 200 °C with a thermal ramp of 12 °C/min, respectively, and NW networks in both samples do not show a significant change in morphology. However, when the AgNW film is annealed at 200 °C for 30 min, some of the NW junctions in Figure 2b are fused or even broken to form Ag droplets (spheroidization).[27,28] This morphological change can be even more significant when the AgNW film is annealed for a longer time, 150 min in Figure 2c. Meanwhile, for the GAgNW film in Figure 2e and f, some of the NW junctions are fused but not broken to disconnect the metallic network during the annealing process. Here, it should be noted that NWs in the circled area in Figure 2e, which are not covered by graphene, are either melted or fused, while those covered by graphene are nearly intact. The metallic network in the GAgNW film does not seem to be influenced by even longer annealing, as it is shown in Figure 2f.

Resistance of the AgNW networks under an atmosphere is measured *in situ* by a two-point probe system during thermal heating and annealing. The resistance values reported in this study represent an average over the surface between two silver strips. In Figure 3, the resistance of the AgNW film during the heating process drops by nearly 1 order of magnitude and slowly, but continuously, further decreases to ~300 Ω during annealing at a constant temperature of 200 °C. After about 60 min of annealing, there is a kink in the resistance of the AgNW

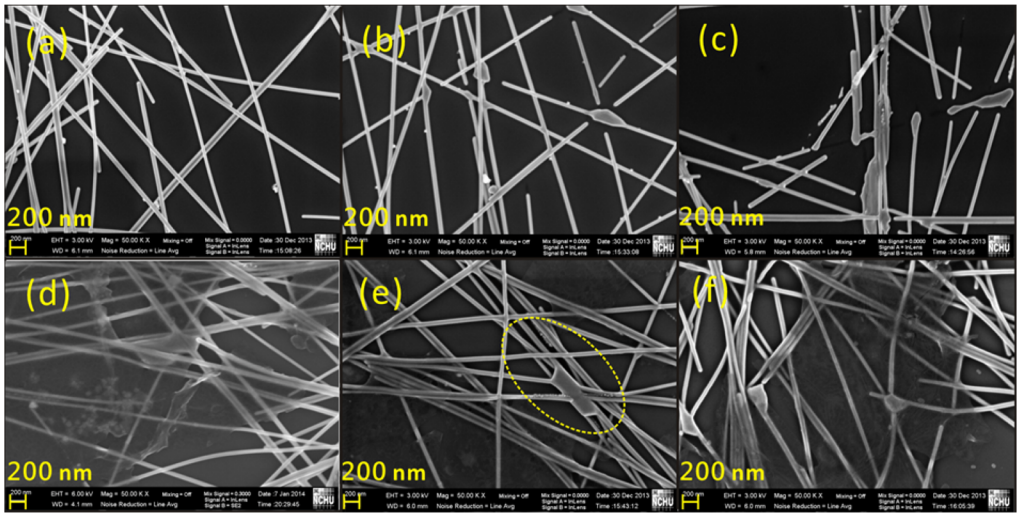

Figure 2. SEM images of AgNW (0.06 wt %) and GAgNW (<0.06 wt %) thin films heated from 25 to 200 °C (a,d) and annealed at 200 °C for 30 min (b,e) and 150 min (c,f), respectively. Circled area in e indicates AgNWs uncovered by the graphene layer.

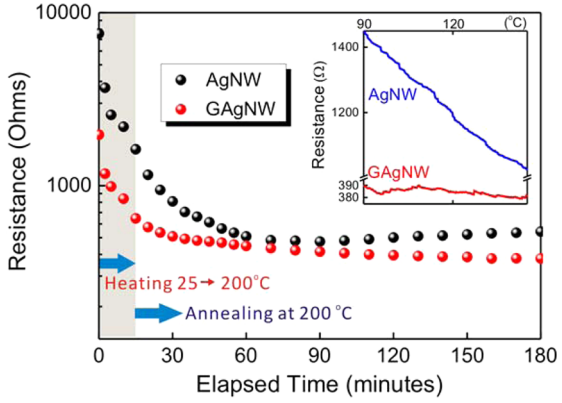

Figure 3. Resistance of AgNW and GAgNW thin films during the heating and annealing process, measured by the two-point probe measurement technique. During the heating process, the temperature of each film increases with a thermal ramp rate of 12 °C/min. The annealing process corresponds to prolonged heating at a constant temperature of 200 °C. The inset shows the resistance measured *in situ* at temperatures ranging from 90 to 150 °C.

film, and the film becomes less conductive, which may be due to the coalescence of the AgNWs.[27] For the GAgNW film, resistance at room temperature is much lower than that of the AgNW film due to graphene. For the GAgNW film, a fast drop of resistance during the heating process is followed by a very slow and continuous decrease during the annealing process, and no kink is observed. This behavior is consistent with the results of the morphological evolution in Figure 2, which shows that AgNW networks covered by graphene are not significantly influenced by high-temperature annealing.

In the inset of Figure 3, the resistance of the AgNW film shows a step-like discrete decreasing behavior at temperatures ranging from 90 to 150 °C, whereas that of the GAgNW film shows relatively small change. This step-like reduction of resistance has been observed for AgNWs during thermal annealing at ≥100 °C, and the efficient contact of NW junctions through the removal of the polyvinylpyrrolidone (PVP) capping layer on AgNW was suggested to be responsible for this behavior.[28] Therefore, the fast drop of resistance for the AgNW film during the heating process can be understood as better ohmic contact and local fusing of uncapped NW junctions that helps to form a higher number of conductive networks. For the GAgNW film, the reduction of resistance may also be attributed to the removal of the polymer capping layer, but in this case, better adhesion occurs not only between NWs but also between NWs and the graphene layer. As the annealing process proceeds, the resistance of the GAgNW film decreases to that of the CVD-grown monolayer graphene,[17] indicating that a highly transparent conductive electrode can be realized from thermally heated subpercolative ($N \lesssim N_c$) GAgNW films, whose resistance is as good as mechanically exfoliated graphene.

To fully understand the details of electrical property evolution during the heating and annealing processes, *in situ* THz conductivities of samples were measured using the THz-TDS technique. The complex electrical conductivity ($\tilde{\sigma}(\omega) = \sigma_1 + i\sigma_2$) of samples is obtained by analyzing the transmitted THz spectra through AgNW and GAgNW films on Si substrates. The THz spectrum through the bare Si substrate was used as a reference. For the GAgNW sample in Figure 4b, $\tilde{\sigma}(\omega)$ shows Drude-like behavior during heating from 25 to 200 °C. By using the simple Drude model, we can obtain the plasma frequency ω_p and the carrier scattering time τ_o.

Due to its subpercolational NW density, $\tilde{\sigma}(\omega)$ of the AgNW film at low temperatures shows non-Drude behavior; σ_1 gradually increases and σ_2 with a negative value decreases as the frequency increases.[8] When the film is heated above 100 °C, however, $\tilde{\sigma}(\omega)$ of the AgNW film begins to show Drude-like behavior, similar to that of the GAgNW film. The non-Drude $\tilde{\sigma}(\omega)$ observed for subpercolative AgNW film cannot be explained by the simple Drude model but then is fitted by the Drude−Smith model. In the Drude−Smith model, the complex conductivity is given by[25]

$$\tilde{\sigma}(\omega) = \frac{\varepsilon_o \omega_p^2 \tau_0}{1 - i\omega\tau_0}\left[1 + \frac{c}{(1 - i\omega\tau_0)}\right] \quad (1)$$

where c is a parameter describing the fraction of the electron's original velocity after some number of scattering events and varies between −1 and 0, corresponding to Drude conductivity for $c = 0$ and complete backscattering for $c = -1$. A negative value of c reflects that the confined electrons within the

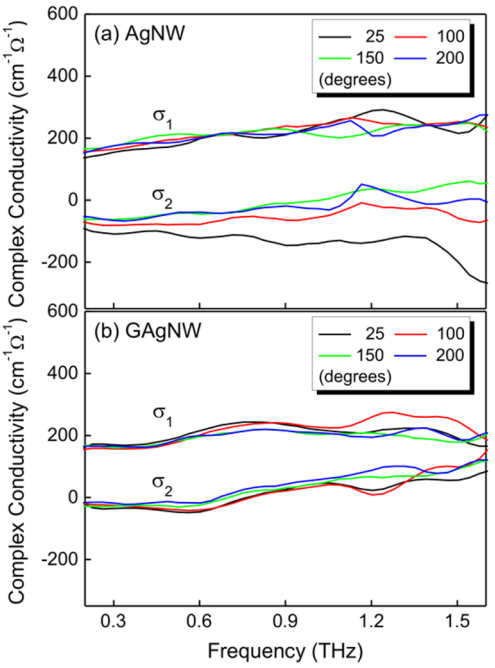

Figure 4. Frequency dependence of complex conductivity of (a) AgNW and (b) GAgNW films measured at temperatures of 25, 100, 150, and 200 °C. Nonconductive AgNW film transfers to conductive when heated above 150 °C.

individual NWs may experience a preferential backward scattering.

In Figure 5, we illustrate the transient behavior of fitting parameters (c, ω_p, and τ_o) and DC conductivity ($= \varepsilon_0\omega_p^2\tau_o(1 + c)$) obtained from AgNW and GAgNW films under similar heating and annealing conditions to those of two-point probe measurement. During continuous heating from 25 to 200 °C (shaded area), the negative c value of the AgNW film increases from −0.8 to −0.6, indicating that better adhesivity between NWs reduces the carrier scattering at the junctions. The plasma frequency ω_p decreases as the AgNW film is heated, whereas the scattering time τ_o increases at a temperature around 100–150 °C. We suggest that this unusual temperature dependence of ω_p and τ_o for the AgNW film is related with the transitional behavior of the subpercolational AgNW network. As the NWs are heated, uncapping of AgNWs followed by fusing at the junctions improves ohmic contact between NWs, and then the critical NW density for the percolative network can be shifted to a lower value. In a separate study, we indeed found that N_c where the metal–insulator transition occurs is shifted from 0.075 wt % to 0.06 wt % when the AgNW film is annealed at T = 135 °C for 5 min.[26] In addition, near the percolational threshold, a slight reduction of ω_p and a rapid increase of τ_o have been observed for metallic networks.[8,29] Therefore, the temperature dependence of ω_p and τ_o during the heating process in Figure 5 corresponds to the transitional behavior of the AgNW film from subpercolative to percolative near the threshold density. Meanwhile, during the annealing process, reduced (increased) ω_p (τ_o) retains a similar value until significant spheroidization occurs at near t = 200 min, which is consistent with the results of two-point probe measurement in Figure 2.

This transitional behavior is not observed in the AgNW film above percolation ($N \sim 0.08$ wt %; open circles in Figure 5), in which ω_p slightly increases with the increase of temperature and τ_o is barely changed. For the originally percolative networks, uncapping of AgNWs at the elevated temperature enhances the electrical conductivity by increasing the number of photoconductive carriers through networks, similar to the effect of increasing NW density.[29] Meanwhile, the scattering time τ_o which corresponds to that of the metallic component in

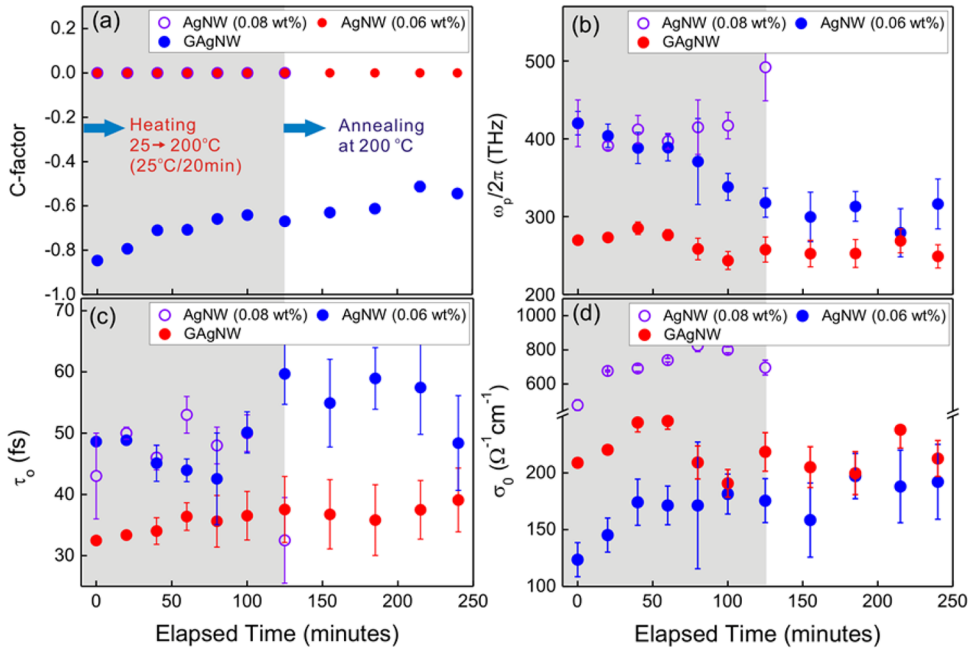

Figure 5. Best-fit parameters, (a) c-factor, (b) plasma frequency, (c) carrier scattering time, and (d) DC conductivity calculated from *in situ* THz-TDS data during the thermal heating and annealing processes. Data points within the first 125 min are measured during heating from 25 to 200 °C, and those at later times are measured during thermal annealing at a constant temperature of 200 °C. The fitting parameters of AgNW films are obtained by using the Drude–Smith model, while those of graphene/AgNW films are obtained by using the Drude model.

inhomogeneous percolative media is nearly independent of thermal heating.[30]

Figure 5b and c also illustrate the temperature dependence of ω_p and τ_o of GAgNW film. Due to the loss of AgNWs during the process of transferring graphene, the accurate estimation of AgNW density in GAgNW film is difficult so that the initial values of ω_p and τ_o at 25 °C in the GAgNW film can vary upon samples. As shown in Figure 5d, the GAgNW film is more conductive than the subpercolative AgNW film, indicating that the main conduction in this film is due to the electron transport along graphene. The overall temperature-dependent variations of physical parameters for the GAgNW film are small, and the thermally induced transitional behavior of subpercolative AgNW film is not observed. As the SEM image in Figure S2 shows, stamp-transferred graphene used in GAgNW film has many defects and disruptions, but our results exhibit that this poor quality stamp-transferred graphene can still efficiently dissipate the heat and keep the AgNW underlayer below the fusing temperature. A slight increase of τ_o in the GAgNW hybrid film in Figure 5c may be due to the improvement of adhesivity between graphene and uncapped AgNWs at the elevated temperature.

As we observed in the above discussion, when the density of AgNWs used in the GAgNW film increases above N_c, percolative AgNW networks rather than the graphene layer would dominate the conduction process in the GAgNW film, and then higher electrical conduction can be achieved not only by increasing the density of AgNWs but also by simply heating the film at a proper temperature. Thermally induced conductivity enhancement, however, has the advantage of maintaining high optical transparency. In addition, since a single-layer graphene is sufficient to improve the thermal stability in the GAgNW film, optical transparency of the GAgNW film can be only 2−3% lower than that of AgNW films. Then our results demonstrate that highly transparent conductive metal NW electrodes with excellent thermal stability can be realized from these graphene-incorporated AgNW hybrid films.

CONCLUSIONS

The thermal evolution of the electrical and physical properties of the AgNW and graphene−AgNW hybrid films was comprehensively characterized by *in situ* THz-TDS and two-point probe measurement. Thermal heating of AgNWs at 90−150 °C could remove the polymer protection coating on AgNWs and improve the ohmic contact between NWs. Annealing at 200 °C further reduced the resistance in the AgNW film, but prolonged annealing led to the breakage of NW junctions and the formation of silver droplets. When coupled with subpercolative AgNWs, stamp-transferred graphene reduced the resistance of the heated GAgNW film up to ∼300 Ω and dramatically improved the thermal stability. THz spectroscopy showed that near-percolative AgNW network could transit to the percolative network by thermal heating to 200 °C. THz-TDS also exhibited that the physical parameters of the GAgNW film show only little variation upon thermal heating and annealing, consistent with the results of two-point probe measurement. Finally, this work provides a full understanding on thermal behavior of metallic films and an easy and effective way to improve thermal and electrical properties of the metal nanostructure networks.

EXPERIMENTAL SECTION

Preparation of AgNW Film. For this study, AgNW films with different NW concentrations (0.06 and 0.08 wt %) were prepared by using the spin coating method on Si substrates. AgNWs dispersed in isopropyl alcohol were acquired from Seashell Technology, LLC (AgNW-60) with an average diameter of 60 nm and a length of 10 μm. Films of different densities were fabricated by subsequent dilution to proper concentration with the same solvent. A micropipette was used to drop 50 μL of the AgNW suspension on the Si substrates and then spun-cast at 1200 rpm for 40 s, followed by heating to 90 °C for 3 min to vaporize any residual solvent. In THz-TDS measurement, it is necessary to use Si substrates with high resistance to ensure high transparency in the THz spectral range.

Preparation of Graphene/AgNW Hybrid Film. The fabrication process of the graphene/AgNW hybrid film on a Si substrate is shown in the schematic illustration (Figure S1). A monolayer graphene film was grown using a low-pressure chemical vapor deposition (CVD) process on copper foil at a temperature of 950 °C and under pressures of 0.3 and 0.7 Torr for precursor gas H_2 and CH_4, respectively. A thin polyethylene terephthalate (PET) layer on the Si substrate was pressed on top of the graphene with soft pressure. Silicon gel was used to help the adhesion of graphene on the PET layer. Then the underlying Cu catalyst was etched with ferric chloride ($FeCl_3$) aqueous solution and rinsed with deionized water to remove residual etchant. The Si/PET/graphene film was subsequently stamped onto the as-prepared AgNW film on a Si substrate, and then the supporting Si/PET layer was peeled off to leave a graphene−AgNW film on Si.

Characterization System. The morphologies of AgNW and GAgNW films through the thermal process were analyzed by using field-emission scanning electron microscopy (FE-SEM, Zeiss-Ultra-plus). Optical transmittance was measured using a dual light source and integrating sphere system (U4100, Hitachi Inc.) A barium sulfate coated integrating sphere with a diameter of 6 cm was used to collect the total transmitted light. A two-point probe of resistance was measured by monitoring the resistance across the thermal couple reader connected to a Keithley 2400 source meter while the temperature of the sample was elevated by a commercially available heat-plate (with a 5 × 5 mm^2 square hole at the center) coupled to a DC power supply. Silver paint strips acted as electrical contacts. Therefore, the values of resistance reported in this study represent an average over the surface between two silver strips, which may have a discrepancy with those of sheet resistance measured by using standard four-point probes. The THz conductivities of AgNW films were measured using the THz-TDS technique. Our homemade THz-TDS system is based on THz emission from a photoconductive antenna (Batop GmbH). The normally transmitted THz pulses were detected by free-space electro-optic sampling in a 2-mm-thick ZnTe crystal (EKSMA Optics) as a function of delay time with respect to the optical pump pulse. The excitation of emitter and the probe of the THz signal were achieved with a Ti:sapphire laser (Coherent Inc.), which delivers ∼150 fs optical pulses at a center wavelength of 800 nm.

ASSOCIATED CONTENT

Supporting Information

Schematic of GAgNW fabrication employing the stamping transfer procedure, the tilted SEM image of a GAgNW film, and the energy dispersive X-ray spectroscopy of AgNW films before and after heating process are included in the Supporting Information. This material is available free of charge via the Internet at http://pubs.acs.org.

AUTHOR INFORMATION

Corresponding Author

*Tel: +886-3-5712121. Fax: +886-3-5716631. E-mail: hyahn@mail.nctu.edu.tw.

Notes

The authors declare no competing financial interest.

■ ACKNOWLEDGMENTS

This work was supported by the Ministry of Science and Technology (102-2112-M-009-012-MY3) and the Science Vanguard Research Program (102-2628-M-007-006) in Taiwan.

■ ABBREVIATIONS

NW, nanowire
AgNW, silver nanowire
THz, terahertz
ITO, indium−tin oxide
THz-TDS, THz time-domain spectroscopy
FE-SEM, field-emission scanning electron microscopy
GAgNW, graphene−silver nanowire

■ REFERENCES

(1) Sun, Y.; Xia, Y. Large-scale Synthesis of Uniform Silver Nanowires Through a Soft, Self-Seeding Polyol Process. *Adv. Mater.* **2002**, *14*, 833−837.
(2) Lee, J.-Y.; Connor, S. T.; Cui, Y.; Peumans, P. Solution-Processed Metal Nanowire Mesh Transparent Electrodes. *Nano Lett.* **2008**, *8*, 689−692.
(3) De, S.; Higgins, T. M.; Lyons, P. E.; Doherty, E. M.; Nirmalraj, P. N.; Blau, W. J.; Boland, J. J.; Coleman, J. N. Silver Nanowire Networks as Flexible, Transparent, Conducting Films: Extremely High DC to Optical Conductivity Ratios. *ACS Nano* **2009**, *3*, 1767−1774.
(4) Hu, L.; Kim, H. S.; Lee, J.-Y.; Peumans, P.; Cui, Y. Scalable Coating and Properties of Transparent, Flexible, Silver Nanowire Electrodes. *ACS Nano* **2010**, *4*, 2955−2963.
(5) Zhu, R.; Chung, C.-H.; Cha, K. C.; Yang, W.; Zheng, Y. B.; Zhou, H.; Song, T.-B.; Chen, C.-C.; Weiss, P. S.; Li, G.; Yang, Y. Fused Silver Nanowires with Metal Oxide Nanoparticles and Organic Polymers for Highly Transparent Conductors. *ACS Nano* **2011**, *5*, 9877−9882.
(6) Leem, D. S.; Edwards, A.; Faist, M.; Nelson, J.; Bradley, D. C.; deMello, J. C. Efficient Organic Solar Cells with Solution-Processed Silver Nanowire. *Adv. Mater.* **2011**, *23*, 4371−4375.
(7) Chung, C.-H.; Song, T.-B.; Bob, B.; Zui, R.; Yang, Y. Solution-Processed Flexible Transparent Conductors Composed of Silver Nanowire Networks Embedded in Indium Tin Oxide Nanoparticle Matrices. *Nano Res.* **2012**, *5*, 805−814.
(8) Tsai, Y.-J.; Chang, C.-Y.; Lai, Y.-C.; Yu, P.; Ahn, H. Realization of Metal−Insulator Transition and Oxidation in Silver Nanowire Percolating Networks by Terahertz Reflection Spectroscopy. *ACS Appl. Mater. Interfaces* **2014**, *6*, 630−635.
(9) Elechiguerra, J. L.; Larios-Lopez, L.; Liu, C.; Garcia-Gutierrez, D.; Camacho-Bragado, A.; Yacaman, M. J. Corrosion at the Nanoscale: The Case of Silver Nanowires and Nanoparticles. *Chem. Mater.* **2005**, *17*, 6042.
(10) Khaligh, H. H.; Goldthorpe, I. Failure of Silver Nanowire Transparent Electrodes Under Current Flow. *Nanoscale Res. Lett.* **2013**, *8*, 235.
(11) Lee, J.-Y.; Connor, S. T.; Cui, Y.; Peumans, P. Solution-Processed Metal Nanowire Mesh Transparent Electrodes. *Nano Lett.* **2008**, *8*, 689.
(12) Corkum, S.; A tes, E. S.; Unalan, H. E. Optimization of Silver Nanowire Networks for Polymer Light Emitting Diode Electrodes. *Nanotechnology* **2013**, *24*, 125202.
(13) Balandin, A. A.; Ghosh, S.; Bao, W.; Calizo, I.; Teweldebrhan, D.; Miao, F.; Lau, C. N. Superior Thermal Conductivity of Single-Layer Graphene. *Nano Lett.* **2008**, *8*, 902.
(14) Nan, H. Y.; Ni, Z. H.; Wang, J.; Zafar, Z.; Shi, Z. X.; Wang, Y. Y. The Thermal Stability of Graphene in Air Investigated by Raman Spectroscopy. *J. Raman Spectrosc.* **2013**, *44*, 1018.
(15) Balandin, A. A. Thermal Properties of Graphene and Nanostructured Carbon Materials. *Nat. mater.* **2011**, *10*, 569.
(16) Chen, S.; Brown, L.; Levendorf, M.; Cai, W.; Ju, S.-Y.; Edgeworth, J.; Li, X.; Magnuson, C. W.; Velamakanni, A.; Piner, R. D.; Kang, J.; Park, J.; Ruoff, R. S. Oxidation Resistance of Graphene-Coated Cu and Cu/Ni Alloy. *ACS Nano* **2011**, *5*, 1321.
(17) Lee, D.; Lee, H.; Ahn, Y.; Jeong, Y.; Lee, D.-Y.; Lee, Y. Highly Stable and Flexible Silver Nanowire−Graphene Hybrid Transparent Conducting Electrodes for Emerging Optoelectronic Devices. *Nanoscale* **2013**, *5*, 7750.
(18) Nair, R. R.; Blake, P.; Grigorenko, A. N.; Novoselov, K. S.; Booth, T. J.; Stauber, T.; Peres, N. M. R.; Geim, A. K. Fine Structure Constant Defines Visual Transparency of Graphene. *Science* **2008**, *320*, 1308.
(19) Lee, M.-S.; Lee, K.; Kim, S.-Y.; Lee, H.; Park, J.; Choi, K.-H.; Kim, H.-K.; Kim, D.-G.; Lee, D.-Y.; Nam, S.-W.; Park, J.-U. High-Performance, Transparent, and Stretchable Electrodes Using Graphene−Metal Nanowire Hybrid Structures. *Nano Lett.* **2013**, *13*, 2814−2821.
(20) Jeong, C.; Nair, P.; Khan, M.; Lundstrom, M.; Alam, M. A. Prospects for Nanowire-Doped Polycrystalline Graphene Films for Ultratransparent Highly Conductive Electrodes. *Nano Lett.* **2011**, *11*, 5020−5025.
(21) Kholmanov, I. N.; Magnuson, C. W.; Aliev, A. E.; Li, H.; Zhang, B.; Suk, J. W.; Zhang, L. L.; Peng, E.; Mousavi, S. H.; Khanikaev, A. B.; Piner, R.; Shvets, G.; Ruoff, R. S. Improved Electrical Conductivity of Graphene Films Integrated with Metal Nanowires. *Nano Lett.* **2012**, *12*, 5679−5683.
(22) Zhu, Y.; Sun, Z.; Yan, Z.; Jin, Z.; Tour, J. M. Rational Design of Hybrid Graphene Films for High-Performance Transparent Electrodes. *ACS Nano* **2011**, *5*, 6472−6479.
(23) Chen, J.; Bi, H.; Sun, S.; Tang, Y.; Zhao, W.; Lin, T.; Wan, D.; Huang, F.; Zhou, X.; Xie, X.; Jiang, M. Highly Conductive and Flexible Paper of 1D Silver-Nanowire-Doped Graphene. *ACS Appl. Mater. Interfaces* **2013**, *5*, 1408−1413.
(24) Dadrasnia, E.; Garet, F.; Lee, D.; Coutaz, J.-L.; Baik, S.; Lamela, H. Electrical Characterization of Silver Nanowire-Graphene Hybrid Films from Terahertz Transmission and Reflection Measurements. *Appl. Phys. Lett.* **2014**, 011101.
(25) Smith, N. V. Classical Generalization of the Drude Formula for the Optical Conductivity. *Phys. Rev. B* **2001**, *64*, 155106−4.
(26) Tsai, Y.-J. Investigation of the Percolation Threshold and the Thermal Stability in Silver Nanowire by THz Reflection Spectroscopy. Master Thesis, The National Chiao Tung University, July 2014.
(27) Woo, J. S.; Han, J. T.; Jung, S.; Jang, J. I.; Kim, H. Y.; Jeong, H. J.; Jeong, S. Y.; Baeg, K.-J.; Lee, G.-W. Electrically Robust Metal Nanowire Network Formation by In-Situ Interconnection with Single-Walled Carbon Nanotubes. *Sci. Rep.* **2014**, *4*, 4804.
(28) Langley, D.; Lagrange, M.; Nguyen, N. D. In Transparent Conductive Oxides and Related Compounds. *Proceedings of the Materials Research Society*, San Francisco, U.S.A., Apr. 21−25, **2014**.
(29) Walther, M.; Cooke, D. G.; Sherstan, C.; Hajar, M.; Freeman, M. R.; Hegmann, F. A. Terahertz Conductivity of Thin Gold Films at the Metal-Insulator Percolation Transition. *Phys. Rev. B: Condens. Matter Mater. Phys.* **2007**, *76*, 125408−9.
(30) Bittar, A.; Berthier, S.; Lafait, J. Mean Field Theory and Scaling Laws for the Optical Properties of Inhomogeneous Media. *J. Phys. (Paris)* **1987**, *48*, 601−610.